Received: 26 September 2018 | Revised: 10 December 2018 | Accepted: 11 December 2018

DOI: 10.1002/pat.4534

RESEARCH ARTICLE

WILEY polymers advanced technologies

Influence type of natural rubber on properties of green biodegradable thermoplastic natural rubber based on poly(butylene succinate)

Parisa Faibunchan[1] | Skulrat Pichaiyut[1] | Wannarat Chueangchayaphan[1] | Claudia Kummerlöwe[2] | Norbert Venneman[2] | Charoen Nakason[1]

[1] Department of Rubber Technology, Faculty of Science and Industrial Technology, Prince of Songkla University, Surat Thani Campus, Surat Thani, Thailand

[2] Faculty of Engineering and Computer Science, Osnabrück University of Applied Sciences, Osnabrück, Germany

Correspondence
Charoen Nakason, Department of Rubber Technology, Faculty of Science and Industrial Technology, Prince of Songkla University, Surat Thani Campus, 84000 Surat Thani, Thailand.
Email: charoen.na@psu.ac.th

Funding information
Thailand Research Fund (TRF), Grant/Award Number: PHD/0208/2557

Green biodegradable thermoplastic natural rubber (GB-TPNR) based on simple blend of natural rubber (NR) and poly(butylene succinate) (PBS) was prepared using three NR alternatives: unmodified NR and epoxidized NR with 25- or 50-mol% epoxide (ie, ENR-25 or ENR-50). It was found that ENR-50/PBS blend showed the best compatibility, which resulted in superior mechanical and thermal properties with the highest crystallinity of the PBS phase, on comparing with the ENR-25/PBS and NR/PBS blends. This might be attributed to stronger chemical interactions between the epoxide groups in ENR-50 and the polar functional groups in PBS, which were confirmed by Fourier transform infrared (FTIR). Furthermore, scanning electron microscopy (SEM), atomic force microscopy (AFM), and polarizing optical microscopy (POM) micrographs of ENR-50/PBS blend revealed phase separation with finer-grained cocontinuous structure than in ENR-25/PBS and NR/PBS simple blends. Furthermore, the chemical interactions in ENR-50/PBS blend enhanced the resistance to accelerated weathering.

KEYWORDS

accelerated weathering properties, epoxidized natural rubber, green biodegradable thermoplastic natural rubber (GB-TPNR), poly(butylene succinate), thermal properties

1 | INTRODUCTION

Nowadays, the nondegradable waste from petrochemical-based materials and from vulcanized rubber products is an important environmental concern.[1] This motivates developing alternative materials from renewable resources, in particular biodegradable and recyclable materials. It is noted that thermoplastic elastomers (TPEs) based on biodegradable components are polymeric materials that enable recycling and reprocessing. They have also advantages in both processing and strength properties, as thermoplastics with the elasticity of vulcanized rubber.[2] However, most TPEs have been produced by blending petroleum-based synthetic rubbers, such as ethylene-propylene rubber (EPR), ethylene-propylene-diene monomer (EPDM) rubber/polypropylene (PP),[3] nitrile rubber (NBR)/PP,[4] chloroprene rubber (CR)/PP,[5] and ethylene-1-octene copolymer (EOC)/linear low-density polyethylene (LLDPE).[6] These polymers are not environmentally friendly, as opposed to natural and green polymers such as natural rubber (NR) and other materials based on natural resources.

It has been established that NR is an abundant green renewable natural resource that can be converted to TPEs by blending with various types of thermoplastics, and these products are categorized as "thermoplastic natural rubbers (TPNRs)."[7,8] The advantages of TPNRs over TPEs that are based on synthetic rubbers are being green and environmentally friendly with outstanding dynamic performance, together with good damping and elastic properties. However, some drawbacks of NR products exist, such as poor thermal resistance and incompatibility with polar thermoplastics.[9-11] To overcome these disadvantages, modified NR has been exploited in TPNR materials. It is noted that various chemical modifications to NR have been performed, including NR grafted with various types of polymers, such as

NR-*g*-poly(methyl methacrylate) (NR-*g*-PMMA),[12,13] NR-*g*-polystyrene (NR-*g*-PS),[14] and NR-*g*-*N*-(4-hydroxyphenyl)maleimide (NR-*g*-HPM),[15] along with epoxidation,[16-18] chlorination,[19] and hydrogenation.[20,21] Among the modified NRs, it is mostly epoxidized natural rubber (ENR) that has been used in TPNRs. This might be due to the ENR having good solvent resistance, superior thermal properties, and compatibility with polar thermoplastics.[22] Therefore, various types of TPNRs based on ENR have been prepared, by blending with various thermoplastics including PP,[4] high-density polyethylene (HDPE),[23] poly(methyl methacrylate) (PMMA),[24] and poly(vinyl chloride) (PVC).[25] To develop new green bio-based or biodegradable thermoplastic natural rubber (GB-TPNR) materials, NR and its derivatives could be blended with biodegradable thermoplastics. Typically, these thermoplastics have functional groups susceptible to hydrolysis, for instance, anhydrides, carbonates, amides, urethanes, ureas, esters, or orthoesters.[26]

Poly(butylene succinate) (PBS) is a synthetic polyester synthesized by the polycondensation of 1,4-butanediol and succinic acid.[27-29] PBS is a most attractive biodegradable polyester with good overall properties, including biodegradability, melt processability, and thermal and chemical resistance.[27,28,30] Therefore, PBS is a most interesting biodegradable thermoplastic that could be used to prepare GB-TPNR. Various types of GB-TPNR have been successfully developed and reported. These include the blends of poly(lactic acid) and natural rubber (PLA/NR),[31] poly(lactic acid)/epoxidized natural rubber (PLA/ENR),[32] and polycaprolactone/epoxidized natural rubber (PCL/ENR). These GB-TPNRs provide good processability, reprocessability, excellent degradability, biocompatibility, and high mechanical properties. Therefore, the advantages beyond these GB-TPNR of ENR/PBS blends are enhanced its thermal and chemical resistance while still keeping a good toughness and elasticity, which are important for wide application (such as automotive industry, engineering, and packaging materials).

In this work, GB-TPNR based on blending NR and PBS was prepared by the simple blend technique without curatives. The main aim was to improve mechanical and thermal properties together with biodegradability of the GB-TPNR. Therefore, effect types of the modified NR, in particular of the epoxide content, on various properties of the GB-TPNR were investigated.

2 | EXPERIMENTAL

2.1 | Materials

Table 1 summarizes details of the materials used in preparing GB-TPNRs based on simple blends of NR/PBS. It is noted that the soft or rubber phase in GB-TPNR was alternatively one of three different types of NR: unmodified NR or ENR with epoxide content either 25 or 50 mol% (ie, ENR-25 or ENR-50). On the other hand, the hard phase in GB-TPNR was PBS, Bionolle 1001 MD (blown-film extrusion grade). In addition, Wingstay L was used as the antioxidant in the NR/PBS and ENR/PBS blends.

2.2 | Preparation of NR/PBS and ENR/PBS simple blends

Blending the NR (ie, NR, ENR-25, or ENR-50) with PBS was performed by melt mixing in an internal mixer (CT Internal Mixer, Charoen tut Co, Ltd, Samut Sakhon, Thailand) with a mixing capacity of 500 cm^3. Blending was carried out at 120°C with a rotor speed of 60 rpm and a fixed blend ratio of NR/PBS = 60/40 wt%. The mixing procedures or preparation steps were performed as indicated in Table 2. That is, NR or ENR was first masticated in the presence of Wingstay L (1 phr) for about 4 minutes at 60°C in the internal mixer, to a final temperature of about 80°C. The rubber–Wingstay L mix was then fabricated to a thin about 2- to 3-mm-thick sheet and then conditioned at room temperature for about 24 hours. In the second step, PBS was incorporated into the mixing chamber and rotated in the mixer with a rotor speed of 60 rpm at 120°C for about 4 minutes. After that, the rubber–Wingstay L mix was added into the mixing chamber, and mixing was continued for another 4 minutes until 8 minutes total mixing time. The rubber/PBS blend was then dumped and fabricated

TABLE 1 Characteristics and suppliers of materials used in the preparation of NR/PBS and ENR/PBS blends

Material	Supplier	Characteristics	
NR	Rubber Authority of Thailand (RAOT) (Nakhon Si Thammarat, Thailand)	Specific gravity	0.92
ENR-25	Muang Mai Guthrie Co Ltd (Surat Thani, Thailand)	Specific gravity Epoxidation level, % Specific gravity Ash content, %	0.97 25.09 0.97 0.27
ENR-50	Muang Mai Guthrie Co Ltd (Surat Thani, Thailand)	Specific gravity Epoxidation level, % Specific gravity Ash content, %	1.03 50.05 1.03 0.24
PBS	Showa Denko Co Ltd (Tokyo, Japan)	Specific gravity Melting point, °C Degree of crystallinity, % Glass transition temperature, °C	1.26 114 30–35 −32
Wingstay L	Eliokem Inc (Ohio)	Specific gravity Average molecular weight, g/mol Melting point, °C Ash content, %	1.10 650 115 0.10

Abbreviations: ENR, epoxidized natural rubber; NR, natural rubber; PBS, poly(butylene succinate).

TABLE 2 Preparation steps of NR/PBS and ENR/PBS blends

Step	Time, min	Ingredients	Quantity, phr
1	0.00	Rubber (NR, ENR-25, or ENR-50)	100
	1.00	Wingstay L	1
	4.00	Dump	
2	0.00	PBS	40
	4.00	Rubber + Wingstay L	60
	8.00	Dump	

Abbreviations: ENR, epoxidized natural rubber; NR, natural rubber; PBS, poly(butylene succinate).

on a two-roll mill to form a thin sheet, approximately 2 to 3 mm thick. Finally, the blend was conditioned at room temperature for about 24 hours before testing and characterizing. Test specimens were eventually prepared by compression molding (CT Compression Machine, Charoen tut Co, Ltd, Samut Sakhon, Thailand) at 150°C with 5 minutes preheating, 10 minutes compression, and 20 minutes cooling times.

2.3 | Attenuated total reflection Fourier transform infrared spectroscopy

Fourier transform infrared (FTIR) (PerkinElmer Inc, Massachusetts) was exploited to analyze chemical structures of the parent polymers (ie, NR, ENR, and PBS) together with NR/PBS and ENR/PBS blends. For attenuated total reflection (ATR), the about 3-mm-thick smooth solid samples were placed on the germanium (Ge) crystal surface. It is noted that the sample surfaces must be flat and smooth with good contact between the sample and the crystal. The FTIR was then operated in the wavenumber range from 400 to 4000 cm^{-1} with 4-cm^{-1} resolution and 64 scans per sample.

2.4 | Morphological properties

Three morphological characterization techniques (ie, scanning electron microscopy [SEM], atomic force microscopy [AFM], and polarizing optical microscopy [POM]) were used to analyze the morphological properties of the NR/PBS and ENR/PBS blends. SEM was performed with ZeissSupra-40 VP (Carl Zeiss Microscopy GmbH, Oberkochen, Germany). The samples were first cryogenically cracked in liquid nitrogen to avoid phase deformation during the cracking. Then, NR phase on the sample surface was thoroughly removed by toluene extraction for about 20 minutes at room temperature. The samples were then dried for 48 hours in a vacuum oven and eventually sputtered with gold before SEM examination.

AFM (Nanosurf EasyScan 2 AFM, Nanosurf AG, Liestal, Switzerland) was also used to analyze phase morphologies in the NR/PBS and ENR/PBS blends. The AFM images were acquired in tapping mode (forward scan) at ambient temperature. The samples were first cut with a glass knife under cryogenic conditions at −70°C to prepare a smooth surface before examining with the AFM.

POM (Axioskop 50 ZEISS, Jena, Germany) was also used to characterize crystalline morphologies during heating and cooling of the samples. A thin film (about 0.1 mm thick) was first prepared by cutting with a glass knife at −70°C for producing a smooth surface. The sample was then placed on a glass slide and covered with a glass slip. Then the images at each temperature were recorded. It is noted that the analysis was carried out by heating the sample from room temperature (about 23 ± 2°C) to 140°C with a heating rate of 20°C/min, and was maintained at 140°C for 1 minute before cooling to 80°C with a cooling rate of 5°C/min.

2.5 | Mechanical properties

A universal tensile testing machine (Tinius Olsen, model 10ST, Salfords, England) was used to determine tensile properties of samples at 25 ± 2°C, according to ISO 37. The test specimens were first prepared by die cutting the molded sheet using die C of ISO 37. Stress-strain curves at the constant elongation rate of 200 mm/min were then recorded. Furthermore, 100% modulus, tensile strength, and elongation at break were estimated from the relevant stress-strain curves. In addition, viscoelastic recovery tests were performed by the tensile testing machine. Tension set was tested according to ISO 2285. The specimen was first deformed by stretching at 100% elongation for 10 minutes. Then, the specimen was allowed to relax for 10 minutes and eventually the tension set was determined by Equation 1.

$$\textit{Tension set}\ (\%) = \left(\frac{L - L_0}{L_0}\right) \times 100, \tag{1}$$

where L is the distance between bench marks after 10-minute retraction and L_0 is the original distance between the original bench marks.

Hardness of materials was also determined by a Shore A durometer (Shore, model S1, Instron, Norwood, Massachusetts) according to ISO 868.

2.6 | Thermal properties

Three thermal analysis techniques (ie, dynamic mechanical analysis [DMA], differential scanning calorimetry [DSC], and thermogravimetric analysis [TGA]) were used to analyze the thermal properties of the parent polymers, together with NR/PBS and ENR/PBS blends. The DMA device used was PerkinElmer DMA 8000 (PerkinElmer Inc, Waltham, Massachusetts). The experiment was performed in tension mode under liquid nitrogen at a frequency of 1 Hz, strain amplitude controlled at 0.010 mm, heating rate of 3°C/min, and over the temperature range from −100°C to 100°C. This method allows observing storage modulus (E'), loss modulus (E''), and damping behavior or loss tangent (tan δ = E''/E') at various temperatures.

The DSC device used was Mettler Toledo DSC823e (Schwerzenbach, Zurich, Switzerland). The samples were first heated from −100°C to 200°C with a heating rate of 10 K/min to eliminate the thermal history effects. The temperature was then maintained at 200°C for 3 minutes before cooling down to −100°C at the same rate (10 K/min). This was to determine the crystallization temperature (T_c). The second heating scan was then performed from −100°C to 200°C at the same heating rate. This scan was used to determine glass transition temperature (T_g), melting temperature (T_m), and degree of

crystallinity (X_c) for semicrystalline component in the sample. It is noted that the degree of crystallinity was calculated from Equation 2.[33]

$$\%\ \text{Degree of crystallinity}\ (X_c) = \frac{\Delta H_m}{\Delta H_m^0} \times \frac{100}{W}, \quad (2)$$

where ΔH_m, ΔH_m^o, and W are the melting enthalpy, melting enthalpy for 100% crystalline PBS, which is 110.3 J/g,[33] and the weight fraction (wt%) of PBS in the NR/PBS and ENR/PBS blends, respectively.

TGA was carried out with a thermogravimetric analyzer (TGA-SDTA 851, Mettler Toledo, Zurich, Switzerland). The mass and its rate of change as functions of temperature were determined for the parent polymers and the blend samples. The experiments were carried out under nitrogen atmosphere with 10°C/min heating rate over the temperature range from 25°C to 650°C. Then, oxygen atmosphere was applied to characterize the samples in the temperature range from 650°C to 900°C, with the same heating rate. The maximum rate of mass loss in the TGA thermogram was taken to indicate the decomposition temperature (T_d).

2.7 | X-ray diffractometer

Wide-angle X-ray diffraction (XRD; X'Pert MPD, Philips, the Netherlands) with Cu Kα radiation source was operated at room temperature. The angular scan range from 5° to 40° (2θ) was covered at 2°/min scan rate.

2.8 | Temperature scanning stress relaxation

Thermomechanical behavior of the samples was characterized by temperature scanning stress relaxation (TSSR) using a TSSR meter (Brabender, Duisburg, Germany). The dumbbell-shaped specimens were first prepared by die cutting using die type 5A, according to ISO 527. The sample was then left in the test chamber of TSSR machine with 50% initial strain at 23°C for about 2 hours to allow isothermal relaxation. Then, the sample was heated with a constant heating rate of 2 K/min. The force-temperature curve and relaxation spectrum of each sample were recorded. The rubber index (RI) was also calculated based on the area underneath a normalized force-temperature curve, as an indicator of rubber-like behavior, as follows.[34]

$$RI = \frac{\int_{T_0}^{T_{90}} F/F_0\, dT}{T_{90} - T_0}. \quad (3)$$

2.9 | Accelerated weathering tests

The accelerated weathering test was conducted in a QUV machine (Model QUV/spray, Westlake, Ohio). The samples were first cut into dumbbell shape (die type C) according to ISO 62. The test was performed by alternately exposing the sample in the panels of the QUV and the prohesion chamber, according to ISO 4892-3 Cycle 2. The samples were transferred between the two chambers with three regulated conditions: ultraviolet radiation, moisture, and temperature. It is noted that a QUV test chamber has lamps that provide ultraviolet radiation at 50°C. Furthermore, moisture level was manipulated by forced condensation spraying at 50°C. In addition, temperature was controlled at 50°C. The samples were automatically rotated for about 72 hours through the three exposure conditions, as indicated in Table 3. The weight loss of a sample was calculated from Equation 4.[9]

$$\textit{Weight loss}\ (\%) = \frac{X_i - X_0}{X_0} \times 100, \quad (4)$$

where X_0 and X_i are the initial mass of specimen and the mass of specimen after accelerated weathering test, respectively.

3 | RESULTS AND DISCUSSION

3.1 | ATR-FTIR spectroscopy

Figure 1 shows ATR-FTIR spectra of the parent polymers (NR, ENR, and PBS) and the rubber/PBS blends without and with dimethyl sulfoxide (DMSO) extraction. Also, Table 4 shows peak assignments for the potential peaks in the infrared spectra displayed in Figure 1. It is seen that the pure PBS (Figure 1A) had characteristic absorption peaks at the wavenumbers 806, 1046, 1151, and 1711 cm^{-1}, assigned, respectively, to C—H out of plane bending, O—C—C stretching, C—C stretching, and C=O stretching vibrations.[35,36] In addition, the pure NR had the characteristic absorption peaks of isoprene units at the wavenumbers 840, 1662, 2963, and 3034 cm^{-1} that correspond to =CH out of plane bending vibrations (*cis*-1,4), C=C stretching vibrations, CH_2 symmetric stretching, and =CH stretching vibrations, respectively.[37] Furthermore, two new absorption peaks were observed in the FTIR spectra of pure ENR-25 and ENR-50 at 871 cm^{-1} (ie, asymmetric C—O—C stretching vibrations of epoxirane rings) and at 1244 cm^{-1} assigned to the symmetric C—O stretching vibrations of epoxirane rings.[38,39] Also, it is clear that the peak intensities at 840 and 1662 cm^{-1} decreased with epoxide level in the ENR. This might be attributed to the consumption of double bonds (C=C) in isoprene units of NR by conversion to oxirane rings in ENR.[38,40,41] Moreover, in Figure 1A, the absorption peak at 3034 cm^{-1} (ie, =CH stretching vibrations) has disappeared from the spectrum of ENR-50 but a peak at 1244 cm^{-1} (C—O stretching vibrations) has emerged. This might be due to ENR-50 having more epoxide groups than ENR-25. Figure 1B shows the characteristic FTIR peaks for the various NR/PBS blends before extracting with DMSO. It is clear that

TABLE 3 Steps in the accelerated weathering test by ultraviolet radiation, moisture, and heat, according to ISO 4892-3 Cycle 2

Step	Function	Irradiance, W/m^2	Temperature, °C	Time, h:min
1	UV	0.76	50	8:00
2	Spray	N/A	N/A	0:15
3	Heat	N/A	50	3:45

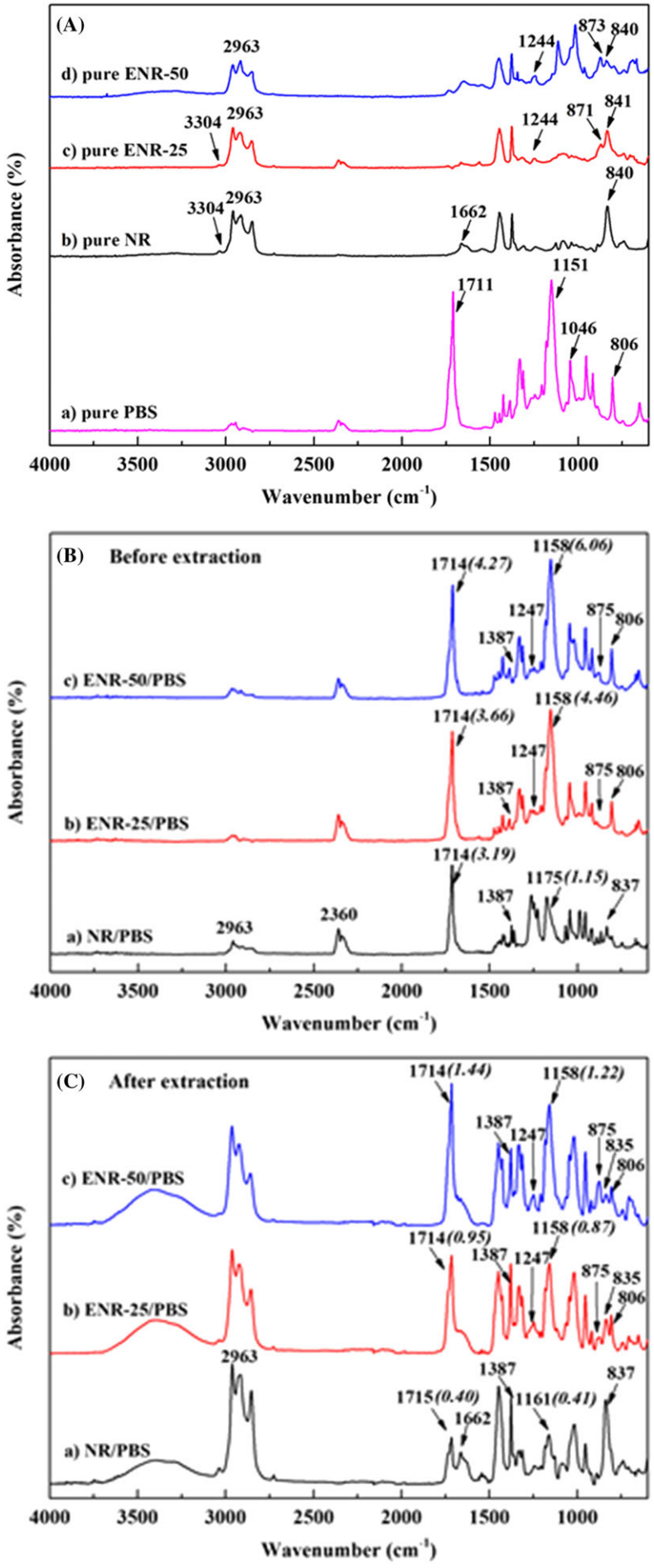

FIGURE 1 A, Attenuated total reflection (ATR)–Fourier transform infrared (FTIR) spectra of the parent polymers (natural rubber [NR], epoxidized natural rubber [ENR], and poly(butylene succinate) [PBS]), B, the rubber/PBS blends, and C, the rubber/PBS blends after extraction in dimethyl sulfoxide (DMSO) [Colour figure can be viewed at wileyonlinelibrary.com]

TABLE 4 Assignments of the FTIR peaks in Figure 1

Assignment	Wavenumber, cm^{-1}						
	PBS	NR	ENR-25	ENR-50	NR/PBS	ENR-25/PBS	ENR-50/PBS
C—H (out of plane bending vibrations)	806	-	-	-	-	806	806
O—C—C stretching vibrations	1046	-	-	-	-	-	-
C—C stretching vibrations	1151	-	-	-	1161	1158	1158
C=O stretching vibrations	1711	-	-	-	1715	1714	1714
—C=H out of plane bending vibrations (*cis*-1,4)	-	840	841	840	837	835	835
C—O—C asymmetric epoxide ring stretching vibrations	-	-	871	873	-	875	875
C—O stretching vibrations	-		1244	1244	-	1247	1247
C=C stretching vibrations	-	1662	-	-	1662	-	-
CH_2 symmetric stretching vibrations	-	2963	2963	-	2963	-	2963
=CH stretching vibrations	-	3034	3034	-	-	-	-

Abbreviations: ENR, epoxidized natural rubber; FTIR, Fourier transform infrared; NR, natural rubber; PBS, poly(butylene succinate).

the NR/PBS blends show the characteristic peaks of both parent polymers. Furthermore, the characteristic peak at wavenumber of 1714 cm^{-1} (ie, C=O stretching vibrations) did not appear in the parent polymers. This peak indicates products of the chemical reaction between epoxide groups in NR and polar functional group in PBS.[42] The peak at wavenumber 1714 cm^{-1} is attributed to ester linkages that formed by the reaction between hydroxyl groups emerging from broken oxirane rings (in ENR molecules) and the functional groups of the polyester. In addition, it is seen that the relative peak intensity at 1714 cm^{-1} of the ENR-50/PBS blend is higher than that of the ENR-25/PBS or NR/PBS blends. This is might be due to more extensive chemical reactions, described here as reaction (1):

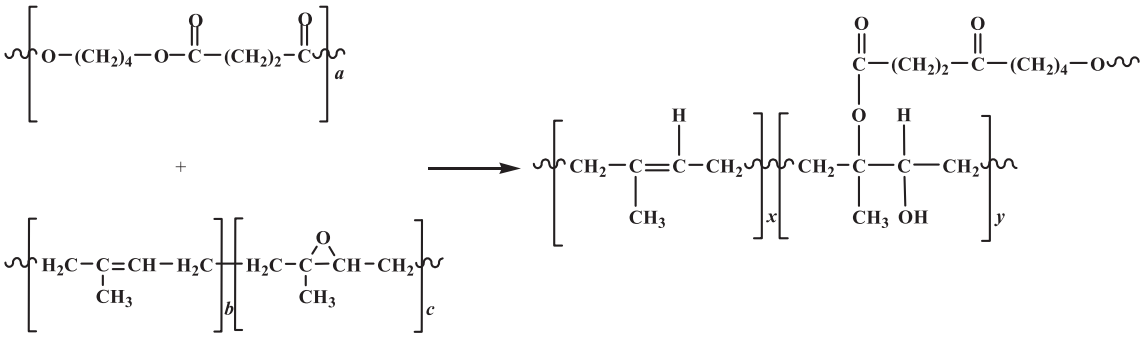

To clarify the chemical interactions of NR and PBS, the NR/PBS blend samples were extracted in DMSO at 190°C for 30 minutes to remove the free PBS phase in the blends. Only the characteristic FTIR absorption peaks for the rubber phase and the reacted PBS phase should remain, as shown in Figure 1C. This corroborates chemical interactions of NR and PBS as well as of ENR and PBS. The relative absorption peak intensities were estimated by normalizing relative to the peak at 2963 cm^{-1} (ie, CH_2 symmetric stretching vibrations).[43] It is seen that the relative intensity at 1714 cm^{-1} (C=O stretching vibrations) for ENR-50/PBS blend (about 1.44) was higher than for ENR-25/PBS (0.95) or NR/PBS (0.40). This corroborates more extensive chemical reactions of epoxide groups in ENR-50 than in ENR-25 or NR, by reactions with the polar functional group in PBS. Meanwhile, it is seen that the relative intensity at 1158 cm^{-1} (C—C stretching vibrations[44]) also increased with epoxidation level. This is attributed to the higher content of —C—C— linkages in ENR and in unextracted or reacted PBS.

3.2 | Morphological properties

Figure 2 shows the SEM and AFM micrographs of the three simple blends of NR/PBS with a fixed blend ratio rubber/PBS = 60/40 wt%. It is clearly seen that the NR/PBS and ENR/PBS simple blends show dual continuous phases or cocontinuous morphology. In addition, the NR/PBS (Figure 2A,D) and ENR-25/PBS blends (Figure 2B,E) show coarser-grained cocontinuous structures than the ENR-50/PBS blend (in Figure 2C,F). Therefore, the ENR-50/PBS blend had the finest-grained cocontinuous phase morphology, with the most interfacial interactions of rubber and PBS phases and the lowest interfacial tension. This might be attributed to higher viscosity nature of ENR led to a higher shear forces during the mixing process that might promote finer cocontinuous phase morphology of the ENR/PBS blend. Furthermore, the chemical interactions of epoxide groups in ENR-50 and polar functional groups in PBS during blending that improved phase compatibility. This result matches well the increased intensity of FTIR peak at wavenumber 1714 cm^{-1} (ie, C=O stretching vibrations). This could be attributed to reaction (1), and a proposed schematic model is shown in Figure 3. It is seen that the unmodified NR/PBS blend has poor interactions and poor phase compatibility. That is, the unmodified NR/PBS blend after extraction in DMSO shows very low FTIR peak intensity at 1714 cm^{-1} but a prominent peak at 1662 cm^{-1} (C=C bonds). This

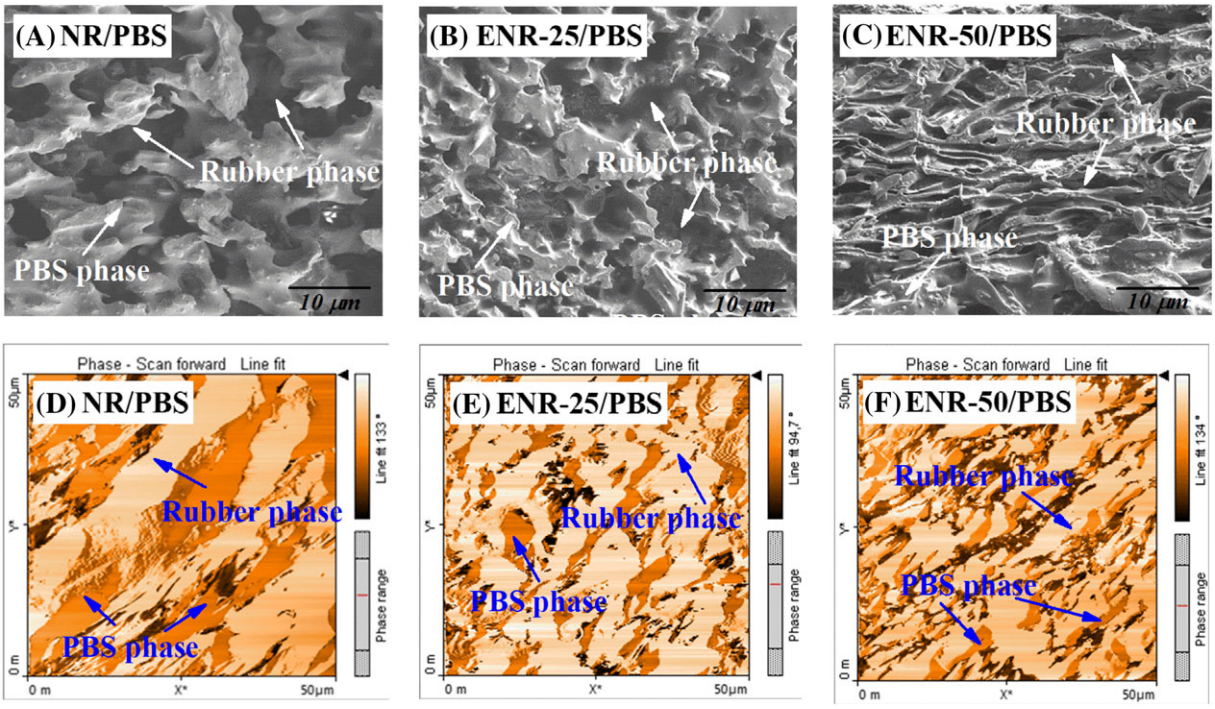

FIGURE 2 Scanning electron microscopy (SEM) micrographs of A, natural rubber (NR)/poly(butylene succinate) (PBS), B, epoxidized natural rubber (ENR)-25/PBS, and C, ENR-50/PBS simple blends together with atomic force microscopy (AFM) micrographs of D, NR/PBS, E, ENR-25/PBS, and F, ENR-50/PBS simple blends with fixed blend proportions rubber/PBS = 60/40 wt% [Colour figure can be viewed at wileyonlinelibrary.com]

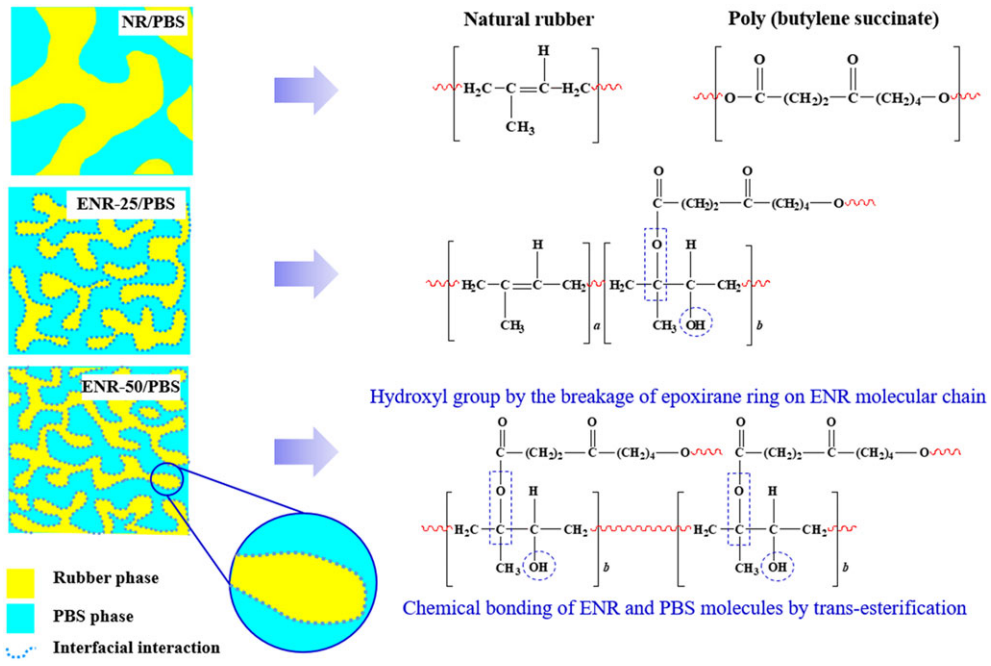

FIGURE 3 A proposed model for the chemical interactions between rubber and poly(butylene succinate) (PBS). ENR, epoxidized natural rubber; NR, natural rubber [Colour figure can be viewed at wileyonlinelibrary.com]

corroborates little chemical interactions of NR and PBS and matches the observed coarse cocontinuous phase morphology. Conversely, the ENR/PBS blends had extensive interactions of the polar functional groups in the two phases. In addition, the extent of chemical interaction increased with epoxidation level of ENR. Hence, the ENR-50/PBS simple blend had the most extensive chemical interactions and the best compatibility, as evidenced by the highest FTIR peak intensity at wavenumber 1714 cm^{-1}. Moreover, the finest cocontinuous phase structure was also observed in the ENR-50/PBS simple blend (Figure 2C,F).

3.3 | Mechanical properties

Figure 4 shows the stress-strain curves of rubber/PBS simple blends with the alternative types of NR (ie, NR, ENR-25, and ENR-50) at the fixed rubber/PBS = 60/40 wt% blend ratio. It can be seen that increasing the epoxide content increased the Young modulus (ie, initial slope of the stress-strain curve) and toughness (ie, area underneath the curve). This indicates improved stiffness and toughness of the blend with epoxidation level. Tensile properties in terms of 100% modulus, tensile strength, and elongation at break were estimated from the stress-strain curves (Figure 4) and are summarized in Table 5 together with data on tension set and hardness. It is clear that the ENR-50/PBS blend shows the highest 100% modulus, tensile strength, and elongation at break. This might be due to more extensive formation of ester linkages, as suggested by the FTIR peak at wavenumber 1714 cm^{-1} in Figure 1B. These mechanical properties can be explained by both chemical interactions at interfaces and good compatibility of ENR and PBS. It is noted that the mechanical properties of NR/PBS and ENR/PBS blends are also strongly affected by the phase morphology. In Figure 2, it is clear that the NR/PBS simple blend shows coarser-grained cocontinuous phases matching the lowest stress-strain curve and related tensile properties (Figure 4). However, the mechanical properties of the blend were considerably enhanced by the finer cocontinuous phase morphology after modification of NR to ENR. In addition, increasing of X_c in ENR-50/PBS blend (Tables 6 and 7) also caused enhancement of the mechanical properties of the blends. Moreover, those properties were improved even more on increasing the epoxide content from 25 to 50 mol%. Therefore, it is concluded that the ENR-50/PBS simple blend had superior

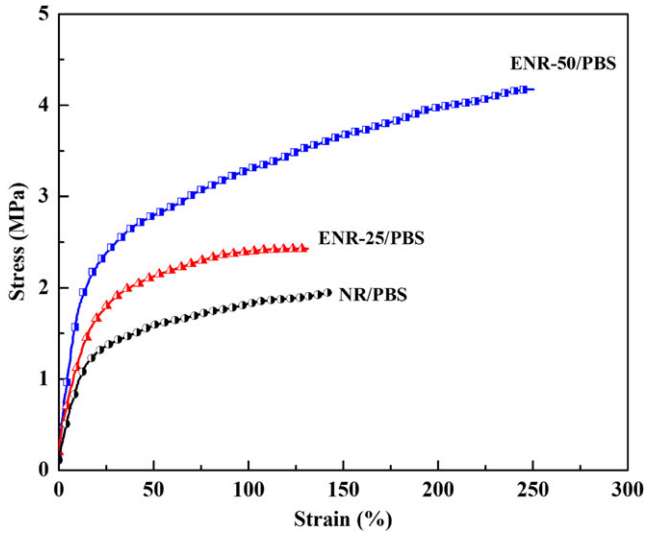

FIGURE 4 Stress-strain curves of the rubber/poly(butylene succinate) (PBS) simple blends with various types of natural rubber and fixed blend proportions rubber/PBS = 60/40 wt%. ENR, epoxidized natural rubber; NR, natural rubber [Colour figure can be viewed at wileyonlinelibrary.com]

TABLE 7 Crystallinity (%) of PBS in natural rubber/PBS simple blends with alternative types of natural rubber and fixed blend proportions rubber/PBS = 60/40 wt%

Sample	A (Peak)	A (Total)	% Crystallinity
NR/PBS	47 804.00	666 952.00	11.22
ENR-25/PBS	75 193.26	614 576.70	12.23
ENR-50/PBS	74 306.16	602 085.10	12.34

Abbreviations: ENR, epoxidized natural rubber; NR, natural rubber; PBS, poly(butylene succinate).

TABLE 5 Mechanical properties of natural rubber/PBS simple blends with alternative types of natural rubber and fixed blend proportions rubber/PBS = 60/40 wt%

Sample	100% Modulus, MPa	Tensile Strength, MPa	Elongation at Break, %	Tension Set, %	Hardness (Shore A)
NR/PBS	1.8 ± 0.09	2.0 ± 0.02	143.4 ± 16.18	65.0 ± 5.0	52.3 ± 5.0
ENR-25/PBS	2.4 ± 0.12	2.5 ± 0.09	124.0 ± 10.34	63.3 ± 5.8	55.3 ± 7.2
ENR-50/PBS	3.3 ± 0.28	4.2 ± 0.71	250.3 ± 18.92	31.7 ± 7.6	56.8 ± 2.7

Abbreviations: ENR, epoxidized natural rubber; NR, natural rubber; PBS, poly(butylene succinate).

TABLE 6 Glass transition temperature (T_g), crystallization temperature (T_c), crystalline melting temperature (T_m), heat of fusion (ΔH_f), and crystallinity (X_c) of the parent polymers (PBS, NR, ENR-25, and ENR-50) and the natural rubber/PBS simple blends with alternative types of natural rubber and fixed blend proportions rubber/PBS = 60/40 wt%

	DMA		DSC					
Sample	T_{g1}, °C	T_{g2}, °C	T_{g1}, °C	T_{g2}, °C	T_c, °C	T_m, °C	ΔH_f, J/g	X_c, %
Pure PBS	−27.6	-	−29.6	-	81.27	116.0	49.2	44.6
Pure NR	-	−59.7	-	−63.2	-	-	-	-
Pure ENR-25	-	−41.7	-	−43.7	-	-	-	-
Pure ENR-50	-	−21.2	-	−21.3	-	-	-	-
NR/PBS	−27.6	−63.5	−29.0	−64.6	82.5	113.5	28.7	52.0
ENR-25/PBS	-	−41.4	-	−44.0	69.8	114.4	31.7	57.5
ENR-50/PBS	-	−23.7	-	−21.5	66.6	115.4	32.4	58.8

Abbreviations: ENR, epoxidized natural rubber; DMA, dynamic mechanical analysis; DSC, differential scanning calorimetry; NR, natural rubber; PBS, poly(butylene succinate).

mechanical properties in terms 100% modulus, tensile strength, and elongation at break, among the blends studied.

In Table 5, it is also seen that the ENR-50/PBS blend shows higher hardness than the alternatives ENR-25/PBS and NR/PBS. This might also be attributed to the epoxide groups in NR having chemical interactions with the polar functional groups in PBS. This matches well the improvements in the Young modulus (ie, stiffness) and tensile properties (Figure 4) together with other mechanical properties (Table 5). Furthermore, the tension set of the blends decreased with epoxide content in ENR. That is, the ENR-50/PBS simple blend exhibited the least tension set, indicating the best overall elastomeric properties. This may be attributed to the chemical reaction of epoxide groups in ENR with polar functional group in PBS and to self-cross-linking of epoxide groups in ENR during mixing, as in the reaction shown in Figure 5. It is noted that the ENR was prepared by chemically modifying NR, by adding epoxide groups. Therefore, ENR possesses relatively high polarity in its molecular structure and can self-cross-link at the opened oxirane rings and by hydrogen bonds or polar interactions, either within one molecule or between neighboring ENR molecules.[22,45-47]

3.4 | Dynamic mechanical analysis

Figure 6 shows the DMA thermograms with storage modulus (E') and tan δ as functions of temperature, for the parent polymers (PBS, NR, ENR-25, and ENR-50) and the NR/PBS simple blends with various types of NR, at the fixed blend proportions rubber/PBS = 60/40 wt%. It can be seen that the storage modulus shows three distinct regions: a glassy high modulus region where the segmental mobility is restricted, a transition region with substantial decrease in E' as temperature increases, and a rubbery region with increasing chain mobility and drastic loss of modulus with increasing temperature. It is noted that the pure PBS shows a narrow transition zone due to its highly crystalline nature, with only a small amount of amorphous regions. In Figure 6A, it is also seen that E' increased in the glassy region with epoxidation level of the NR. This might be due to intermolecular attractions together with chain entanglements that could be corroborated by the Mooney viscosity, shown in Figure 7. It is seen that the pure NR had the least Mooney viscosity, which increased with epoxide content, matching previous studies.[48,49] This may be attributed

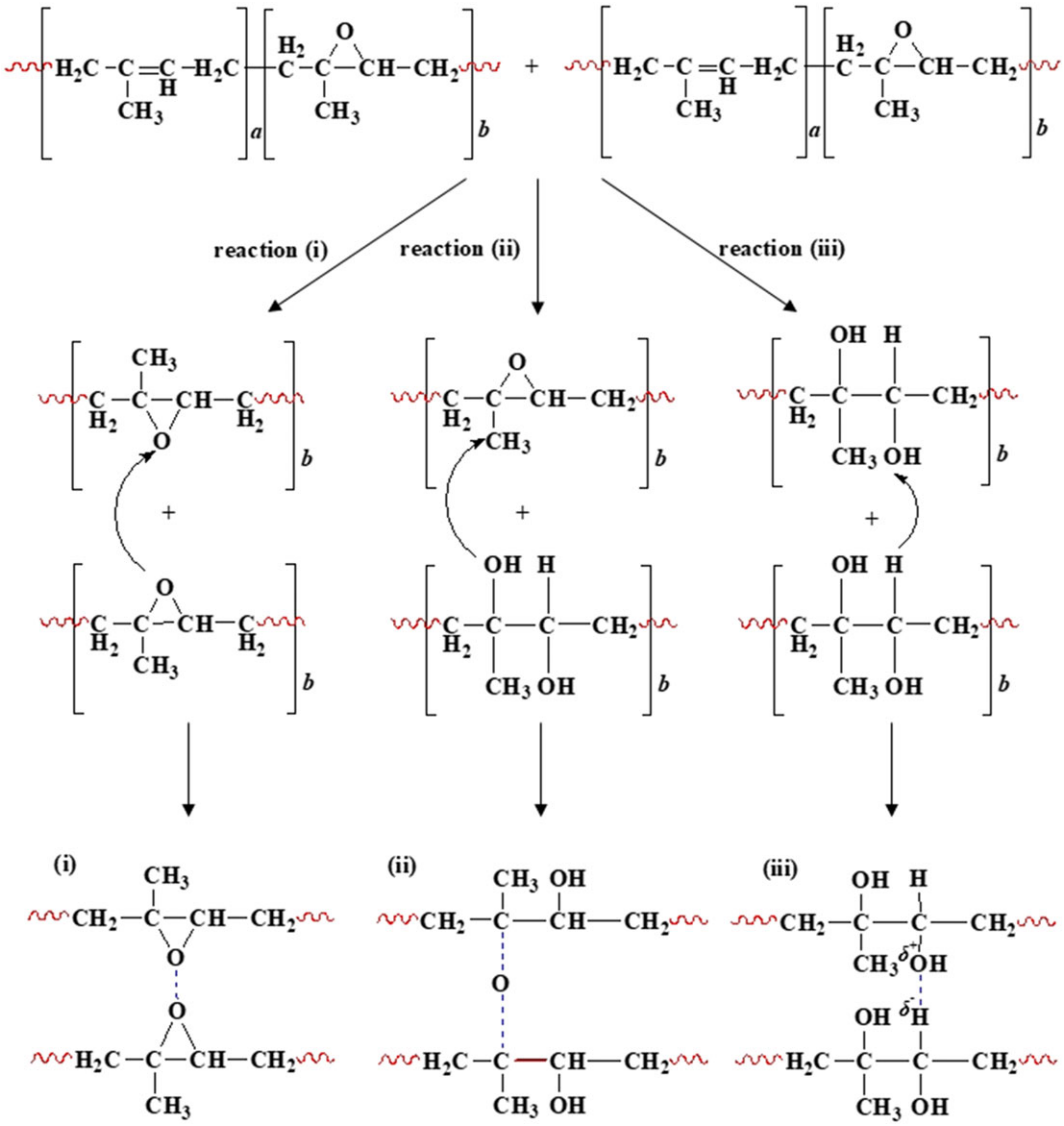

FIGURE 5 Self-cross-linking reactions of epoxidized natural rubber (ENR) via its epoxide groups [Colour figure can be viewed at wileyonlinelibrary.com]

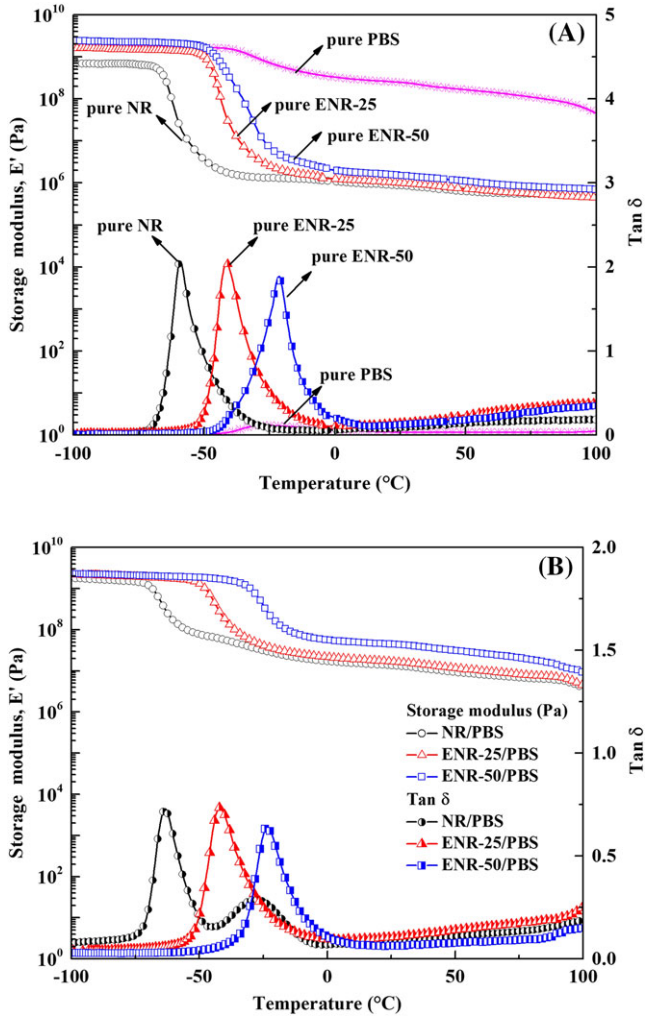

FIGURE 6 Storage modulus and tan δ as functions of temperature (A) for the parent polymers (poly(butylene succinate) [PBS], natural rubber [NR], epoxidized natural rubber [ENR]-25, and ENR-50) and (B) for the natural rubber/PBS simple blends with various types of natural rubber and fixed blend proportions rubber/PBS = 60/40 wt% [Colour figure can be viewed at wileyonlinelibrary.com]

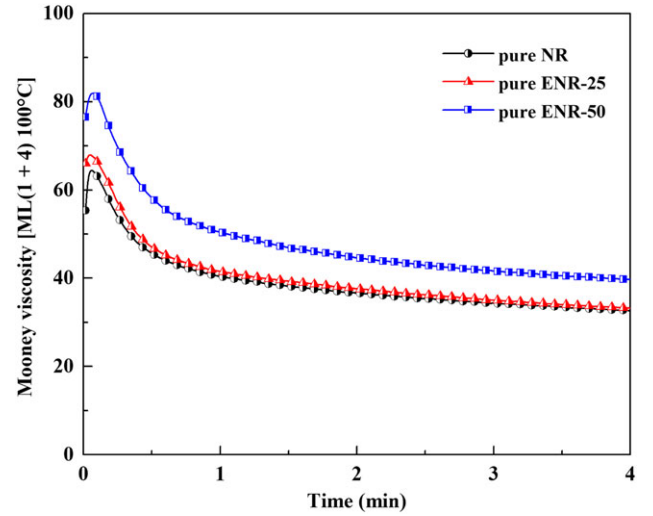

FIGURE 7 Mooney viscosity of pure natural rubber (NR), pure epoxidized natural rubber (ENR)-25, and pure ENR-50, on using large rotor at 100°C [Colour figure can be viewed at wileyonlinelibrary.com]

to self-cross-linking, chemical interactions, and chain entanglements of ENR molecules. In Figure 6B, it can be seen that the ENR-50/PBS blend showed the highest E' of the simple blends. This might be due to stronger intermolecular forces from chemical interactions and attractive forces between ENR-50 and PBS.

In Figure 6A, it is also seen that the pure PBS showed the least area underneath the tan δ curve, which indicates the poorest damping properties; PBS is semicrystalline by nature. On the other hand, the three types of NR had larger areas underneath the tan δ curve than PBS. It is clear that pure NR had the largest area, followed in rank order by ENR-25 and ENR-50. This matches the elasticity and damping properties of these materials. Apart from the chemical differences of various NR types, also, molecular weight (MW) and its distribution are important determinants of elasticity and damping properties. In this work, pure NR had MW of about (1×10^6),[50] which is typically higher than those of pure ENR-25 or pure ENR-50 (ie, approximately 6.8×10^4 and 3.9×10^4).[51] Typically, the tan δ peak indicates the glass transition temperature (T_g).[52] In Figure 6A and Table 6, it is seen that the pure PBS, pure NR, pure ENR-25, and pure ENR-50 had their T_gs at −27.6°C, −59.7°C, −41.7°C, and −21.2°C, respectively. That is, the T_g shifted to higher temperatures with increasing epoxidation level. This might be caused by chain stiffening and the chemical interactions of epoxide functional groups in ENR restricting molecular mobility. In rubber/PBS simple blends (Figure 6 B), it can be seen that the NR/PBS simple blend showed two distinct tan δ peaks corresponding to T_g of NR (−63.5°C) and that of PBS (−27.6°C). In contrast, the ENR-25/PBS and ENR-50/PBS simple blends show only a single T_g peak at about −41.4°C and −23.7°C, respectively. These T_gs are between those of the parent polymers, ENR and PBS. This might be attributed to the T_g of ENR-25 (−41.7°C) and ENR-50 (−21.2°C) overlapping with the T_g of PBS (−27.6°C) to appear as one single tan δ peak and hence a single T_g. This reason is strong rationale for the ENR-50/PBS blend due to smaller difference of T_gs between ENR-50 and PBS (ie, ENR-50 = −21.2°C and PBS = −27.6°C). However, larger difference T_gs between ENR-25 (−41.7°C) and PBS caused suspicious phenomenon of the single T_g. However, according to the morphology in Figure 11, the phase separation to form cocontinuous phase morphology was observed in both ENR-25/PBS and ENR-50/PBS blends. This confirms that a single T_g may not arise from the blend miscibility but shifting of T_gs toward each other and overlapping to form a single tan δ curve and T_g. Similar overlapping of ENR-25 blend was also discovered in our previous work.[9]

3.5 | Differential scanning calorimetry

Figure 8 shows the DSC thermograms for the pure polymers (NR, ENR-25, ENR-50, and PBS) and the NR/PBS simple blends with alternative types of NR, at the fixed blend proportions rubber/PBS = 60/40 wt%. Also, Table 6 shows glass transition temperature (T_g), crystallization temperature (T_c), melting temperature (T_m), ΔH_f, and degree of crystallinity (X_c) for the same cases. In Figure 8A,B and Table 6, it can be seen that the crystallization temperature (T_c) of pure PBS is about 81.27°C. However, T_c of the three types of pure rubber could not

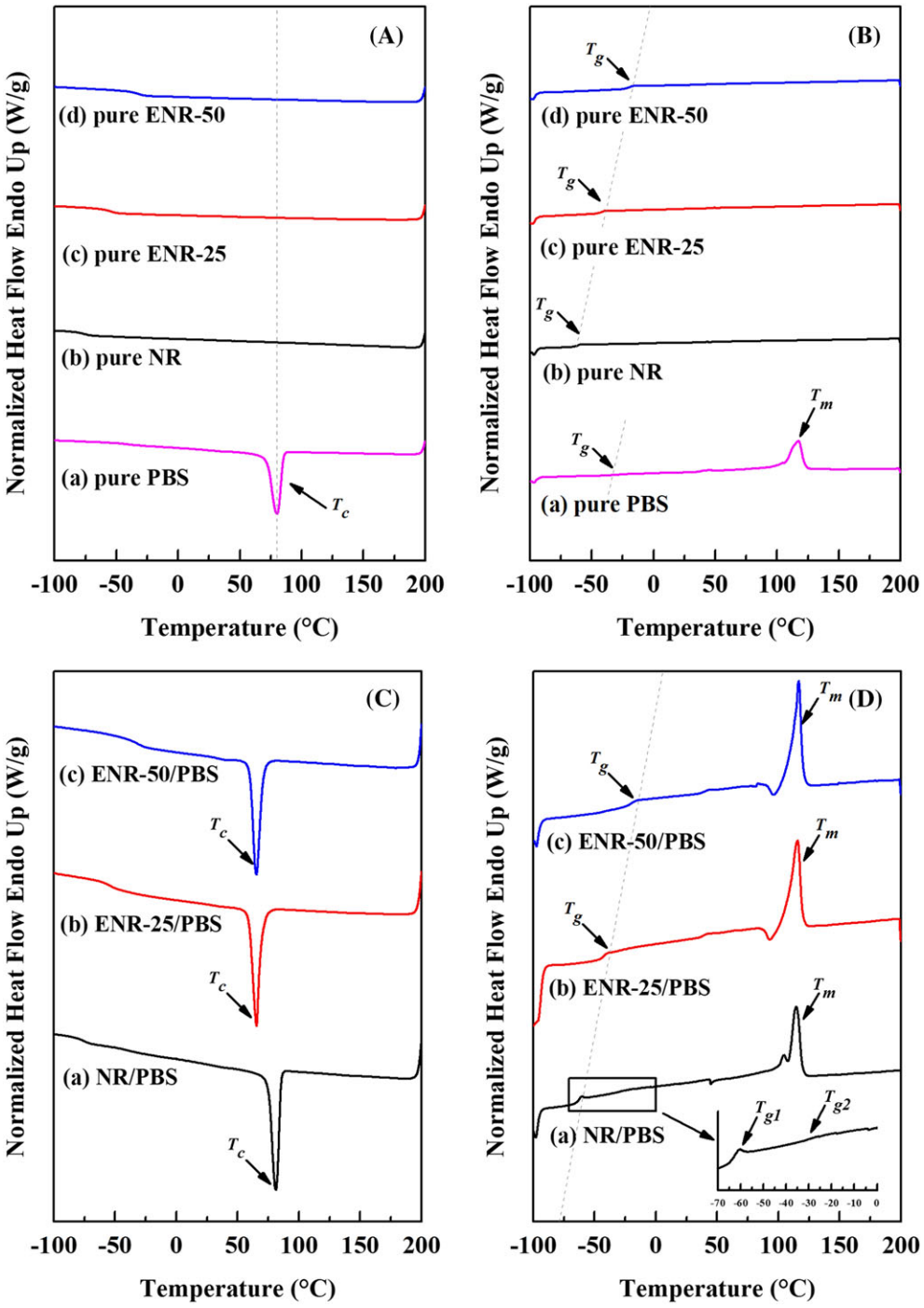

FIGURE 8 Differential scanning calorimetry (DSC) thermograms of the parent polymers (natural rubber [NR], epoxidized natural rubber [ENR]-25, ENR-50, and poly(butylene succinate) [PBS]), A, first cooling scan from 200°C to −100°C and B, second heating scan from −100°C to 200°C, and of the natural rubber/PBS simple blends with various types of natural rubber with fixed blend proportions rubber/PBS = 60/40 wt%, C, first cooling scan from 200°C to −100°C and D, second heating scan from −100°C to 200°C [Colour figure can be viewed at wileyonlinelibrary.com]

be determined due to their amorphous nature. In addition, the T_c of PBS phase in NR/PBS simple blends (Figure 8C) shifted toward lower temperatures with epoxide content of rubber. This might be attributed to increased chemical interactions of polar functional groups forming C—O—C or O—H linkages that decrease T_c of the PBS phase in the rubber/PBS blends.

The glass transition temperature (T_g), crystalline melting temperature (T_m), heat of fusion (ΔH_f), and degree of crystallinity (%X_c) were also estimated from the second heating scan with DSC. In Figure 8B, D and Table 6, it is seen that the T_g of pure PBS, NR, ENR-25, and ENR-50 is −29.6°C, −63.2°C, −43.7°C, and −21.3°C, respectively. Furthermore, the NR/PBS simple blend showed two distinct T_gs, but the ENR/PBS blends had a single T_g, similar to the DMA results (Figure 6 B). In Table 6, it is also seen that the crystalline melting temperature (T_m) of NR/PBS simple blends decreased by about 1°C to 2°C from that of pure PBS. It is noted that the melting peak areas (in Figure 8 B,D) are directly related to the degree of crystallinity (X_c) in PBS phase. It is clearly seen that the degree of crystallinity of PBS phase in the

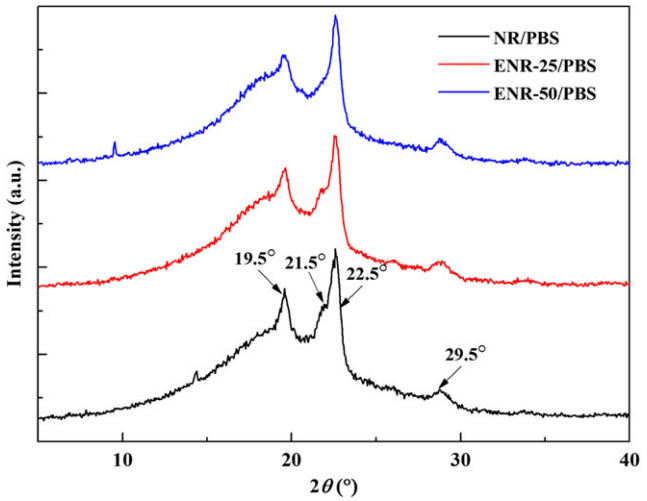

FIGURE 9 The X-ray diffraction (XRD) patterns of natural rubber/poly(butylene succinate) (PBS) simple blends with various natural rubber types and a fixed blend proportions rubber/PBS = 60/40 wt%. ENR, epoxidized natural rubber; NR, natural rubber [Colour figure can be viewed at wileyonlinelibrary.com]

rubber/PBS blends was higher than in pure PBS. This is surprising as the blending could severely disrupt the original crystalline structures and perturb it with the added rubber. However, in this case, the rubber phase carries nonrubber components that might act as nucleating agents, namely, fatty acids and other small molecules: impurities in the NR. These might form nuclei during cooling and initiate and propagate the crystallization of PBS in the rubber/PBS blends.[53-55]

The crystallinity of PBS phase in NR/PBS blend was determined by XRD with results shown in Figure 9 and Table 7. Four strong diffraction peaks are seen at 2θ = 19.5°, 21.5°, 22.5°, and 29.5°. They correspond to the (020), (021), (110), and (111) planes of α-form PBS crystal, respectively.[56,57] The intensities of (020) and (021) planes gradually weakened with epoxidation level of NR, accompanied by a slight increase in the intensity of (110) plane. This may be attributed to the variation of crystallite integrity and crystal growth patterns in PBS phase of the blend, perturbed by the rubber phase. In addition, the degree of crystallinity of rubber/PBS blends is assessed from intensities of the original diffraction peaks (2θ = 19.5°, 21.5°, and 22.5°) for the rubber/PBS blends. In Figure 9 and Table 7, it is seen that the degree of crystallinity PBS increased with epoxidation level. That is, the ENR-50/PBS blends show the most crystallinity, followed by ENR-25/PBS and unmodified NR/PBS blends in this order.

In Table 6, it is also seen that the PBS phase in the ENR-50/PBS simple blend exhibited higher heat of fusion (ΔH_f) and degree of crystallinity (X_c) than ENR-25/PBS or NR/PBS. This might be due to higher degree of crystallinity and blend compatibility of ENR-50 and PBS. This might improve the mechanical properties, storage modulus, and other related properties of the blend (Figures 4 and 6).

3.6 | Thermogravimetric analysis

Figure 10 shows TGA and derivative thermogravimetry (DTG) thermograms of NR/PBS simple blends. Also, Table 8 shows temperatures for

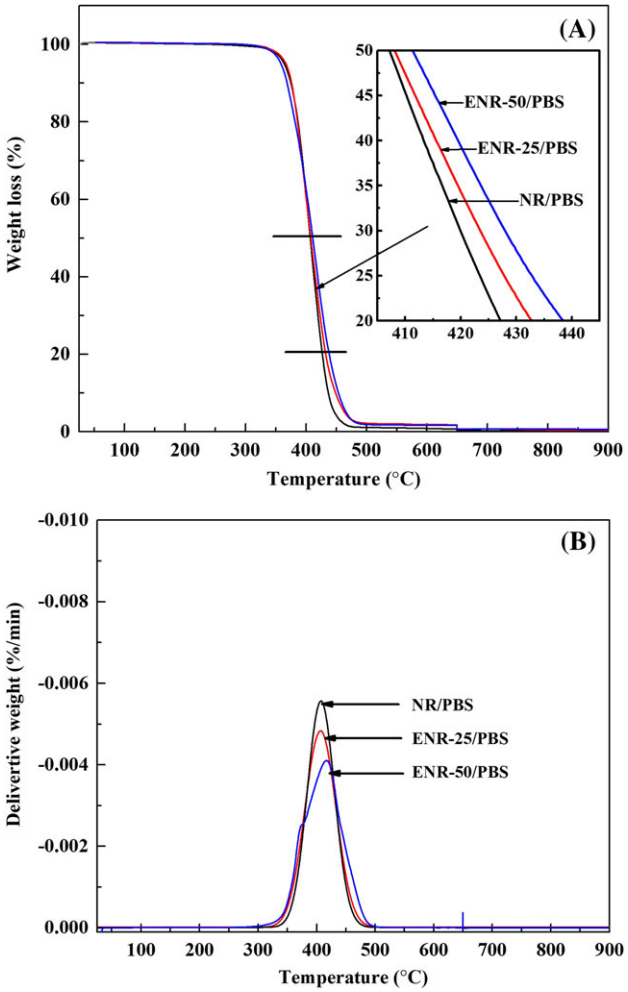

FIGURE 10 A, Thermogravimetry (TGA) thermograms and B, Derivative thermogravimetry (DTG) curves for the natural rubber/poly(butylene succinate) (PBS) simple blends with various natural rubber types and fixed blend proportions rubber/PBS = 60/40 wt% (B). ENR, epoxidized natural rubber; NR, natural rubber [Colour figure can be viewed at wileyonlinelibrary.com]

TABLE 8 Temperature at 5% and 90% weight losses and decomposition temperature (T_d) for the natural rubber/PBS simple blends with fixed blend proportions rubber/PBS = 60/40 wt%

				Weight Loss, %	
Sample	T_5, °C	T_{90}, °C	T_d, °C	At 425°C	At 900°C
NR/PBS	364.0	437.0	406.2	77.1	99.9
ENR-25/PBS	366.7	448.7	407.8	71.8	99.6
ENR-50/PBS	398.0	453.7	419.4	66.6	99.4

Abbreviations: ENR, epoxidized natural rubber; NR, natural rubber; PBS, poly(butylene succinate).

select weight losses and the decomposition temperature (T_d), for the NR/PBS simple blends with fixed blend proportions rubber/PBS = 60/40 wt%. It can be seen that thermal degradation of rubber/PBS blends showed a single degradation step between 300°C and 500°C in nitrogen atmosphere. Furthermore, it is seen that the ENR-50/PBS simple blend showed better thermal degradation resistance than ENR-25/PBS or NR/PBS as indicated by its comparatively high decomposition

temperature (T_d). That is, the decomposition temperature (T_d) of ENR-50/PBS is 419.4°C, while the T_d of ENR-25/PBS is 407.8°C and for NR/PBS, it is 406.2°C (Table 8). The temperatures for 5% and 90% weight losses (T_5 and T_{90}) also increased with epoxidation level for the rubber/PBS simple blends. This might be due to the double bonds in the isoprene units being partly replaced by epoxide groups enabling intermolecular interactions of the ENR.[47] In Table 8, the ENR-50/PBS simple blend has the lowest weight loss at 425°C and at 900°C, with the least area under the DTG peaks. That is, the area under the DTG peak of ENR-50/PBS blend was less than the areas for ENR-25/PBS and NR/PBS. This might be due to the chemical interactions and the finest-grained cocontinuous phase structure (Figure 2).

3.7 | Polarizing optical microscopy

Figure 11 shows the POM micrographs for pure PBS and NR/PBS simple blends with the fixed blend ratio rubber/PBS = 60/40. NR is an amorphous polymer, while PBS is a semicrystalline thermoplastic, as indicated in Figure 11B,C. That is, the PBS crystallizes during cooling from 140°C (Figure 11A) to 90°C (Figure 11B), and higher crystallinity is seen at the lower temperature 80°C (Figure 11C). It is noted that the dark areas indicate amorphous phases, while the bright areas are crystalline phases of PBS in Figure 11D,G,I. Therefore, it is seen that the NR/PBS, ENR-25/PBS, and ENR-50/PBS simple blends were in molten states at 140°C, but cocontinuous phase morphology and the phase interfaces could still be easily distinguished. That is, the NR/PBS simple blend had large cocontinuous phase domains, while finer cocontinuous phase structures were found in the ENR-25/PBS and ENR-50/PBS simple blends. Also, it is seen that the pure PBS at 90°C (Figure 11B) shows spherulitic morphology that resulted in tougher PBS.[58] The size of spherulites is obviously smaller with rubber in the blend (Figure 11E,H,K), leading to a notable improvement in the crystallinity (Table 6) and hence toughness of the blend (Figure 4). Furthermore, at 80°C, the pure PBS (Figure 11C) exhibits fingerprint lines in the micrograph, while the NR/PBS blend shows very clear

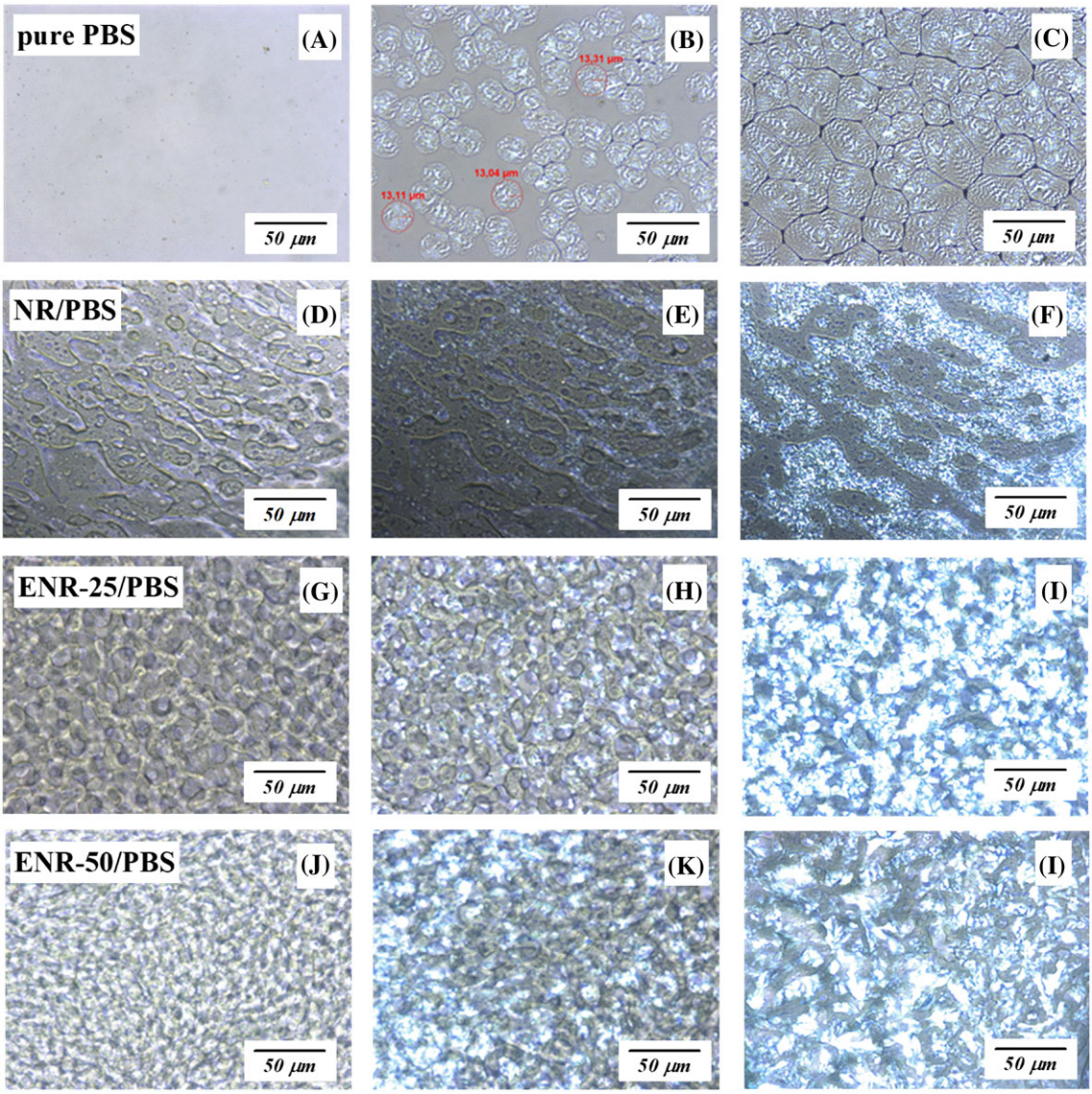

FIGURE 11 Polarized optical micrographs of A–C, pure poly(butylene succinate) (PBS), D–F, natural rubber (NR)/PBS blend, G–I, epoxidized natural rubber (ENR)-25/PBS blend, and J–L, ENR-50/PBS blend, at 140°C, 90°C, and 80°C [Colour figure can be viewed at wileyonlinelibrary.com]

cocontinuous phase structure (Figure 11F,I,L) and the ENR-50/PBS simple blend has the finest grain morphology. This agrees well with the SEM and AFM micrographs in Figure 2. In addition, these results indicate that the NR might nucleate crystallite growth in the PBS phase, as corroborated by the DSC results in Figure 8. Therefore, it is concluded that the crystallinity and morphology could be altered during heating and cooling, as described in the schematic model of Figure 12. That is, the crystallization behavior of a polymer is typically closely related to temperature. In molten state or at melting temperature, crystalline structures are completely converted to amorphous state (Figure 12A). At the crystallization temperature, the regular molecular segments are aligned initiating a crystallite from a small nucleus and eventually expanding until crystallization is completed. In solid state at ambient temperature, the phase-separated morphology includes closely packed regular PBS crystallites in amorphous rubber (Figure 12C).

3.8 | Temperature scanning stress relaxation

Figure 13 shows the normalized force-temperature trace and the relaxation spectrum for the pure rubbers and the various NR/PBS simple blends at the fixed blend proportions rubber/PBS = 60/40 wt%. Also, Table 9 shows initial stress (σ_o), T_x, and RI for the parent polymers (NR, ENR-25, and ENR-50) and the same simple blends. In Figure 13A, it is seen that the force curves of pure ENR-25 and pure ENR-50 showed plateau regions but the curve for pure NR exhibited slight decreasing trend in the temperature ranges of 23°C to 40°C. Then, strong decreases of forces were observed until 80°C. This was indicated by peaks in the relaxation spectra. The plateau region of pure ENR-25 and ENR-50 can be explained by the entropy elastic behavior of the materials presumably caused by dipole-dipole interaction between epoxy groups. In Table 9, it is seen that the initial stresses (σ_o) of parent rubbers were lower than for the rubber/PBS blends. This is attributed to the cocontinuous structure of the rubber/PBS blends that improved strength. Furthermore, higher force-temperature curves for the pure ENR-50 and the pure ENR-25 are seen than for pure unmodified NR. This might be attributed to interactions of polar functional groups in ENR-50 and ENR-25 that enabled self-cross-linking (Figure 5). This matches also E' (Figure 6) and Mooney viscosity (Figure 7). In Figure 13A, two significant relaxation peaks are seen for the pure rubbers. The first peak at about 60°C might be attributed to chemical linkages between nonrubber components (ie, proteins and fatty acids) in NR that cause storage hardening.[59-61] Also, the physical interactions of polar moieties in rubber might contribute to the first peak.[62] The second relaxation peak in the temperature range 120°C to 140°C might be due to the degradation of linkages in rubber phase and scission of polymer main chains together with the opening of oxirane rings. In Figure 13B and Table 9, it is also seen that the ENR-50/PBS simple blend had higher T_{10} than the ENR-25/PBS or NR/PBS simple blends. This relates to higher moduli, stiffness, and tensile properties of the blends (Table 5) and to E' (Figure 6). This indicates improved thermal resistance of the blends with the polar functional groups of ENR by chemical interactions. In Figure 13B, it is also seen that the rubber/PBS simple blends exhibited two relaxation peaks. The first peak may indicate melting of PBS crystallites at about 90°C, based on the crystallization temperature estimates from POM (Figure 11) and DSC (Figure 8). Furthermore, the second peak at about 115°C indicates the melting of blend components to form a molten polymer mix. Furthermore, in Table 9, RI of ENR-50/PBS blend was higher than those of ENR-25/PBS and NR/PBS simple blends. It is noted that RI is a measure of

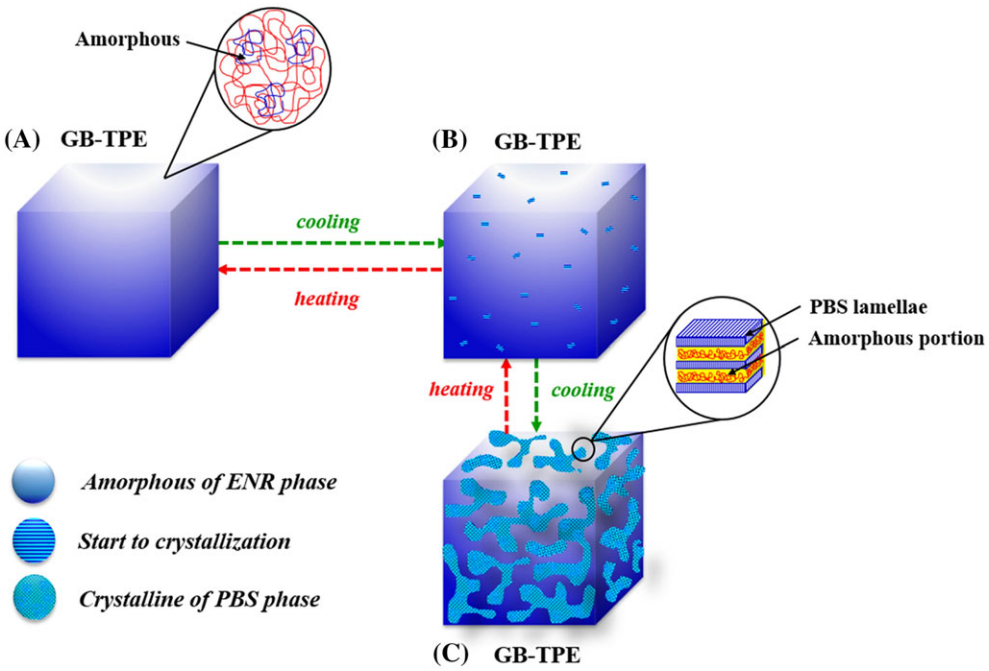

FIGURE 12 Schematic microstructure in natural rubber/poly(butylene succinate) (PBS) simple blend at different states: A, heating, B, crystallization at about 90°C (Table 6), and C, solid state at a low temperature. ENR, epoxidized natural rubber; GB-TPE, green biodegradable thermoplastic elastomer [Colour figure can be viewed at wileyonlinelibrary.com]

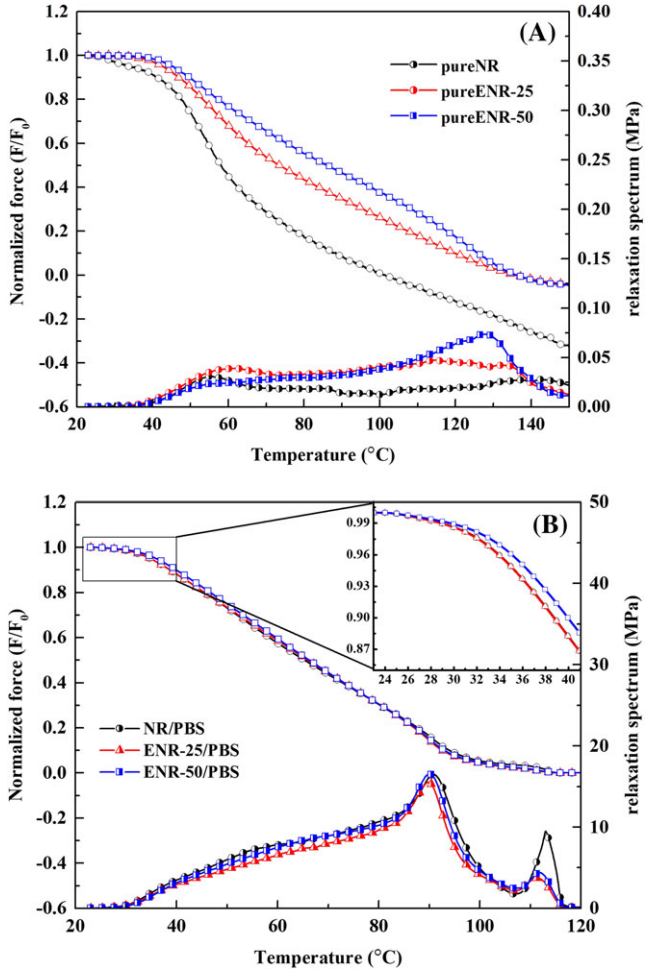

FIGURE 13 Normalized force-temperature traces and relaxation spectra A, for the pure rubbers (natural rubber [NR], epoxidized natural rubber [ENR]-25, and ENR-50) and B, for the natural rubber/poly(butylene succinate) (PBS) simple blends with various types of natural rubber and fixed blend proportion rubber/PBS = 60/40 wt% [Colour figure can be viewed at wileyonlinelibrary.com]

TABLE 9 Initial stress (σ_o), T_x, and rubber index (*RI*) for the pure rubbers (NR, ENR-25, and ENR-50) and the natural rubber/PBS simple blends with alternative types of natural rubber and fixed blend proportions rubber/PBS = 60/40 wt%

		Temperature, °C			
Sample	σ_o, MPa	T_{10}	T_{50}	T_{90}	*RI*
Pure NR	0.02	40.9	58.1	87.3	0.47
Pure ENR-25	0.03	46.9	73.4	119.6	0.58
Pure ENR-50	0.03	49.7	86.0	126.0	0.62
NR/PBS	7.12	38.8	65.3	94.0	0.61
ENR-25/PBS	6.03	38.8	66.0	92.6	0.62
ENR-50/PBS	6.58	39.9	66.3	93.0	0.63

Abbreviations: ENR, epoxidized natural rubber; NR, natural rubber; PBS, poly(butylene succinate).

rubber-like behavior, and higher RI value indicates better elasticity. The ENR-50/PBS blends had the highest RI and hence were the most elastic. This matches well the high elongation at break (Figure 4 or Table 5) together with low tension set (Table 5), incurred by the epoxide groups in the blend.

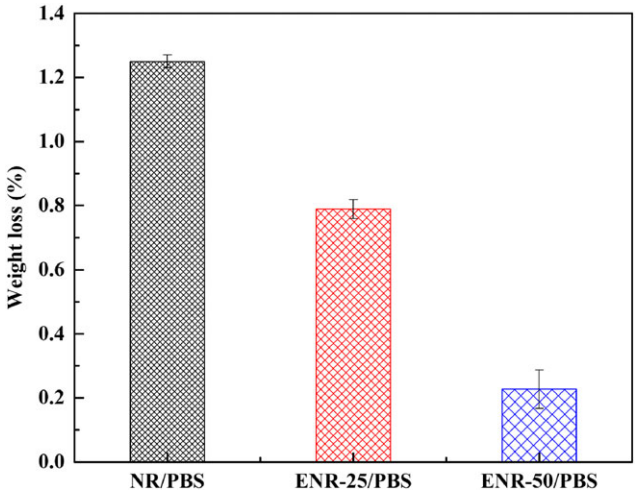

FIGURE 14 Weight loss from accelerated weathering for the natural rubber (NR)/poly(butylene succinate) (PBS), epoxidized natural rubber (ENR)-25/PBS, and ENR-50/PBS simple blends with fixed blend proportions rubber/PBS = 60/40 wt% [Colour figure can be viewed at wileyonlinelibrary.com]

3.9 | Accelerated weathering tests

The accelerated weathering tests of rubber/PBS simple blends were conducted in a QUV machine according to ISO 62. Figure 14 shows the weight losses of the NR/PBS, ENR-25/PBS, and ENR-50/PBS blends during accelerated weathering. It is seen that the NR/PBS blend had the highest weight loss, while the ENR-25/PBS blend exhibited less weight losses and the ENR-50/PBS blend had the least loss. That is, the weight loss decreased with epoxide group content. This may be attributed to the molecular characteristics and to interactions of rubber and PBS that gave the strongest structure to the ENR-50/PBS simple blend with the finest-grained cocontinuous phase morphology. In addition, the crystallinity may also affect the degradation of a blend.[42] That is, the PBS phase in ENR-50/PBS had the highest crystallinity, while the NR/PBS blend had the lowest (Table 6). This is presumably because the crystalline regions are more difficult to degrade than the amorphous portion. Therefore, polymer blends with low crystallinity and chemical interactions between the phases are more susceptible to degradation.

4 | CONCLUSIONS

Various properties of GB-TPNR based on NR and PBS blends with alternative types of rubber were investigated. Mechanical, dynamic mechanical, and thermal stability properties and thermomechanical and damping behavior were studied. It was found that ENR with 50-mol% epoxide (ie, ENR-50) provided the best properties in a rubber/PBS simple blend, superior to ENR-25 or unmodified NR. This is attributed to the chemical interactions of epoxide groups in ENR-50 and the polar functional groups in PBS, confirmed by FTIR. Furthermore, ENR-50/PBS blend had the finest-grained morphology, as confirmed by SEM, AFM, and POM. Moreover, the crystallinity of PBS was highest in the ENR-50/PBS blend, which may have contributed to the superior

properties of this blend. We also found that the crystallinity of PBS in the rubber/PBS blends increased with epoxidation level of ENR, according to DSC and XRD. This indicates that the crystallinity of PBS in rubber/PBS blends played an important role in controlling various properties, including mechanical and thermal properties, stress relaxation, and resistance to accelerated weathering. Furthermore, the accelerated weathering test was exploited to confirm that the blend with high degree of interactions between rubber and PBS phases, together with fine-grained cocontinuous phase morphology, had superior degradation resistance with the least weight loss from weathering.

ACKNOWLEDGEMENTS

This study was supported by research grants from the Royal Golden Jubilee (RGJ) PhD Program (grant no. PHD/0208/2557), the Thailand Research Fund (TRF). Dr Charoen Nakason as principal researcher and Miss Parisa Faibunchan as the research assistant also would like to express their gratitude to the Faculty of Science and Industrial Technology, Prince of Songkla University, Surat Thani Campus. Regarding German collaborators, we gratefully acknowledge the facility support from the Faculty of Engineering and Computer Science, University of Applied Sciences Osnabrück, Germany, and the Erasmus program for financial support. In addition, we would like to thank Assoc Prof Dr Seppo Karrila for assistance with manuscript preparation.

ORCID

Charoen Nakason https://orcid.org/0000-0003-1631-9369

REFERENCES

1. Wu K-J, Wu C-S, Chang J-S. Biodegradability and mechanical properties of polycaprolactone composites encapsulating phosphate-solubilizing bacterium *Bacillus* sp. PG01. *Process Biochem*. 2007;42(4):669-675.
2. Riahi F, Benachour D, Douibi A. Dynamically vulcanized thermoplastic elastomer blends of natural rubber and polypropylene. *Int J Polym Mater*. 2004;53(2):143-156.
3. Ibrahim A, Dahlan M. Thermoplastic natural rubber blends. *Prog Polym Sci*. 1998;23(4):665-706.
4. Coran A, Patel R. Rubber-thermoplastic compositions. Part VIII. Nitrile rubber polyolefin blends with technological compatibilization. *Rubber Chem Technol*. 1983;56(5):1045-1060.
5. Salmah H, Azra B, Yusrina M, Ismail H. A comparative study of polypropylene/(chloroprene rubber) and (recycled polypropylene)/(chloroprene rubber) blends. *J Vinyl Addit Techn*. 2015;21(2):122-127.
6. Rocha MCG, Leyva ME, Oliveira MGD. Thermoplastic elastomers blends based on linear low density polyethylene, ethylene-1-octene copolymers and ground rubber tire. *Polymer*. 2014;24(1):23-29.
7. Nakason C, Wannavilai P, Kaesaman A. Effect of vulcanization system on properties of thermoplastic vulcanizates based on epoxidized natural rubber/polypropylene blends. *Polym Test*. 2006;25(1):34-41.
8. Nakason C, Worlee A, Salaeh S. Effect of vulcanization systems on properties and recyclability of dynamically cured epoxidized natural rubber/polypropylene blends. *Polym Test*. 2008;27(7):858-869.
9. Pichaiyut S, Wisunthorn S, Thongpet C, Nakason C. Novel ternary blends of natural rubber/linear low-density polyethylene/thermoplastic starch: influence of epoxide level of epoxidized natural rubber on blend properties. *Iran Polym J*. 2016;25(8):711-723.
10. Kalkornsurapranee E, Yung-Aoon W, Thongnuanchan B, Thitithammawong A, Nakason C, Johns J. Influence of grafting content on the properties of cured natural rubber grafted with PMMAs using glutaraldehyde as a cross-linking agent. *Adv Polym Tech*. 2017;37(5):1478-1485.
11. Nakason C, Saiwari S, Kaesaman A. Rheological properties of maleated natural rubber/polypropylene blends with phenolic modified polypropylene and polypropylene-g-maleic anhydride compatibilizers. *Polym Test*. 2006;25(3):413-423.
12. Kalkornsurapranee E, Sahakaro K, Kaesaman A, Nakason C. From a laboratory to a pilot scale production of natural rubber grafted with PMMA. *J Appl Polym Sci*. 2009;114(1):587-597.
13. Kochthongrasamee T, Prasassarakich P, Kiatkamjornwong S. Effects of redox initiator on graft copolymerization of methyl methacrylate onto natural rubber. *J Appl Polym Sci*. 2006;101(4):2587-2601.
14. Asaletha R, Kumaran M, Thomas S. Thermal behaviour of natural rubber/polystyrene blends: thermogravimetric and differential scanning calorimetric analysis. *Polym Degrad Stab*. 1998;61(3):431-439.
15. Nakason C, Sasdipan K, Kaesaman A. Novel natural rubber-*g*-*N*-(4-hydroxyphenyl)maleimide: synthesis and its preliminary blending products with polypropylene. *Iran Polym J*. 2014;23(1):1-12.
16. Alwaan I, Hassan A. Effects of zinc borate loading on thermal stability, flammability, crystallization properties of magnesium oxide/(90/10) mLLDPE/(NR/ENR-50) blends. *Iran Polym J*. 2014;23(4):277-287.
17. Ooi ZX, Ismail H, Bakar AA. Study on the ageing characteristics of oil palm ash reinforced natural rubber composites by introducing a liquid epoxidized natural rubber coating technique. *Polym Test*. 2014;37:156-162.
18. Saramolee P, Lopattananon N, Sahakaro K. Preparation and some properties of modified natural rubber bearing grafted poly(methyl methacrylate) and epoxide groups. *Eur Polym J*. 2014;56:1-10.
19. Zhong JP, Li SD, Wei YC, Peng Z, Yu HP. Study on preparation of chlorinated natural rubber from latex and its thermal stability. *J Appl Polym Sci*. 1999;73(14):2863-2867.
20. Mahittikul A, Prasassarakich P, Rempel G. Noncatalytic hydrogenation of natural rubber latex. *J Appl Polym Sci*. 2007;103(5):2885-2895.
21. Tangthongkul R, Prasassarakich P, Rempel GL. Hydrogenation of natural rubber with Ru $[CH=CH(Ph)]Cl(CO)(PCy_3)_2$ as a catalyst. *J Appl Polym Sci*. 2005;97(6):2399-2406.
22. Gelling IR. Epoxidised natural rubber. *J Natural Rubber Res*. 1991;6(3):184-205.
23. Nakason C, Jarnthong M, Kaesaman A, Kiatkamjornwong S. Thermoplastic elastomers based on epoxidized natural rubber and high-density polyethylene blends: effect of blend compatibilizers on the mechanical and morphological properties. *J Appl Polym Sci*. 2008;109(4):2694-2702.
24. Nakason C, Panklieng Y, Kaesaman A. Rheological and thermal properties of thermoplastic natural rubbers based on poly(methyl methacrylate)/epoxidized-natural-rubber blends. *J Appl Polym Sci*. 2004;92(6):3561-3572.
25. Mousa A, Ishiaku U, Ishak ZM. Rheological properties of dynamically vulcanized poly(vinyl chloride)/epoxidized natural rubber thermoplastic elastomers: effect of processing variables. *Polym Test*. 2000;19(2):193-204.
26. Li S. Hydrolytic degradation characteristics of aliphatic polyesters derived from lactic and glycolic acids. *J Biomed Mater Res*. 1999;48(3):342-353.
27. Ray SS, Okamoto K, Okamoto M. Structure and properties of nanocomposites based on poly(butylene succinate) and organically modified montmorillonite. *J Appl Polym Sci*. 2006;102(1):777-785.
28. Song L, Qiu Z. Crystallization behavior and thermal property of biodegradable poly(butylene succinate)/functional multi-walled carbon nanotubes nanocomposite. *Polym Degrad Stab*. 2009;94(4):632-637.
29. Doi Y, Kasuya K-i, Abe H, et al. Evaluation of biodegradabilities of biosynthetic and chemosynthetic polyesters in river water. *Polym Degrad Stab*. 1996;51(3):281-286.

30. Uesaka T, Nakane K, Maeda S, Ogihara T, Ogata N. Structure and physical properties of poly(butylene succinate)/cellulose acetate blends. *Polymer*. 2000;41(23):8449-8454.

31. Tanrattanakul V, Bunkaew P, Boonlong N. Influence of rubber mastication on mechanical properties of poly(lactic acid)-based thermoplastic natural rubber. *J Biobaased Mater Bioenergy*. 2012;6(5):573-579.

32. Wang Y, Chen K, Xu C, Chen Y. Supertoughened biobased poly(lactic acid)–epoxidized natural rubber thermoplastic vulcanizates: fabrication, co-continuous phase structure, interfacial in situ compatibilization, and toughening mechanism. *J Phys Chem*. 2015;119(36):12138-12146.

33. Wahit MU, Hassan A, Ibrahim AN, Zawawi NA, Kunasegeran K. Mechanical, thermal and chemical resistance of epoxidized natural rubber toughened polylactic acid blends. *Sains Malaysiana*. 2015;44(11):1615-1623.

34. Norbert V. Characterization of thermoplastic elastomers by means of temperature scanning stress relaxation measurements. In: *Thermoplastic Elastomers*. China: InTech; 2012:347-370.

35. Siracusa V, Lotti N, Munari A, Dalla RM. Poly(butylene succinate) and poly(butylene succinate-co-adipate) for food packaging applications: gas barrier properties after stressed treatments. *Polym Degrad Stab*. 2015;119:35-45.

36. Zheng L, Li C, Zhang D, Guan G, Xiao Y, Wang D. Multiblock copolymers composed of poly(butylene succinate) and poly(1,2-propylene succinate): effect of molar ratio of diisocyanate to polyester-diols on crosslink densities, thermal properties, mechanical properties and biodegradability. *Polym Degrad Stab*. 2010;95(9):1743-1750.

37. Rolere S, Liengprayoon S, Vaysse L, Sainte-Beuve J, Bonfils F. Investigating natural rubber composition with Fourier transform infrared (FT-IR) spectroscopy: a rapid and non-destructive method to determine both protein and lipid contents simultaneously. *Polym Test*. 2015;43:83-93.

38. Salaeh S, Nakason C. Influence of modified natural rubber and structure of carbon black on properties of natural rubber compounds. *Polym Compos*. 2012;33(4):489-500.

39. Wichian AN. Preparation and mechanical property of the epoxidized natural rubber from field latex. *Rubber Thai J*. 2013;2:1-8.

40. Nakason C, Kaesaman A, Klinpituksa P. Preparation, thermal and flow properties of epoxidized natural rubber. *Songkla J Sci Techn*. 2001;23:415-424.

41. Van Zyl AJ, Graef SM, Sanderson RD, Klumperman B, Pasch H. Monitoring the grafting of epoxidized natural rubber by size-exclusion chromatography coupled to FTIR spectroscopy. *J Appl Polym Sci*. 2003;88(10):2539-2549.

42. Faibunchan P, Nakaramontri Y, Chueangchayaphan W, et al. Novel biodegradable thermoplastic elastomer based on poly(butylene succinate) and epoxidized natural rubber simple blends. *J Polym Environ*. 2018;26:1-14.

43. Nakaramontri Y, Nakason C, Kummerlöwe C, Vennemann N. Influence of modified natural rubber on properties of natural rubber–carbon nanotube composites. *Rubber Chem Technol*. 2015;88(2):199-218.

44. Llorens E, Ibañez H, Del Valle L, Puiggalí J. Biocompatibility and drug release behavior of scaffolds prepared by coaxial electrospinning of poly(butylene succinate) and polyethylene glycol. *Mater Sci Eng C*. 2015;49:472-484.

45. Hamzah R, Bakar MA, Dahham OS, Zulkepli NN, Dahham SS. A structural study of epoxidized natural rubber (ENR-50) ring opening under mild acidic condition. *J Appl Polym Sci*. 2016;133(43):1-13. https://doi.org/10.1002/app.44123

46. Ng S-C, Gan L-H. Reaction of natural rubber latex with performic acid. *Eur Polym J*. 1981;17(10):1073-1077.

47. Nakason C, Kaewsakul W, Kaesaman A. Thermoplastic natural rubbers based on blending of ethylene-vinyl acetate copolymer with different types of natural rubber. *J Elastom Plast*. 2012;44(1):89-111.

48. Rohadi AA, Rahmat AR, Kamal MM. Effect of epoxidation level in silica filled epoxidized natural rubber compound on cure, rheological, mechanical and dynamic properties. *Appl Mech Mater*. 2014;554:71-75. Trans Tech Publications

49. Kinasih N, Fathurrohman M, Winarto D. Swelling behaviour in n-pentane and mechanical properties of epoxidized natural rubber with different epoxide content. *Mater Sci Eng A*. 2017;223(1):012002. IOP Publishing

50. Johnson T, Thomas S. Effect of epoxidation on the transport behaviour and mechanical properties of natural rubber. *Polymer*. 2000;41(20):7511-7522.

51. Poh B, Yong A. Effect of molecular weight of epoxidized-natural rubber on viscosity and tack of pressure-sensitive adhesives. *J Appl Polym Sci*. 2010;115(2):1120-1124.

52. Liu X, Dever M, Fair N, Benson R. Thermal and mechanical properties of poly(lactic acid) and poly(ethylene/butylene succinate) blends. *J Environ Polym Degr*. 1997;5(4):225-235.

53. Gent A, Kawahara S, Zhao J. Crystallization and strength of natural rubber and synthetic *cis*-1,4-polyisoprene. *Rubber Chem Technol*. 1998;71(4):668-678.

54. Gent A, Zhang LQ. Strain-induced crystallization and strength of elastomers. I. *cis*-1,4-polybutadiene. *J Polym Sci Pol Phys*. 2001;39(7):811-817.

55. Zhou Y, Kosugi K, Yamamoto Y, Kawahara S. Effect of non-rubber components on the mechanical properties of natural rubber. *Polym Advan Technol*. 2017;28(2):159-165.

56. Ihn K, Yoo E, Im S. Structure and morphology of poly(tetramethylene succinate) crystals. *Macromolecules*. 1995;28(7):2460-2464.

57. Dong T, He Y, Zhu B, Shin K-M, Inoue Y. Nucleation mechanism of α-cyclodextrin-enhanced crystallization of some semicrystalline aliphatic polymers. *Macromolecules*. 2005;38(18):7736-7744.

58. Wang H, Gan Z, Schultz JM, Yan S. A morphological study of poly(butylene succinate)/poly(butylene adipate) blends with different blend ratios and crystallization processes. *Polymer*. 2008;49(9):2342-2353.

59. Wu M, Heinz M, Vennemann N. Investigation of un-vulcanized natural rubber by means of temperature scanning stress relaxation measurements. *Adv Mat Res*. 2013;718:117-123. Trans Tech Publications

60. Vennemann N, Schwarze C, Kummerlöwe C. Determination of crosslink density and network structure of NR vulcanizates by means of TSSR. *Adv Mat Res*. 2014;844:482-485. Trans Tech Publications

61. Sookyung U, Nakason C, Thaijaroen W, Vennemann N. Influence of modifying agents of organoclay on properties of nanocomposites based on natural rubber. *Polym Test*. 2014;33:48-56.

62. Matchawet S, Kaesaman A, Vennemann N, Kummerlöwe C, Nakason C. Optimization of electrical conductivity, dielectric properties, and stress relaxation behavior of conductive thermoplastic vulcanizates based on ENR/COPA blends by adjusting mixing method and ionic liquid loading. *Ind Eng Chem Res*. 2017;56(13):3629-3639.

How to cite this article: Faibunchan P, Pichaiyut S, Chueangchayaphan W, Kummerlöwe C, Venneman N, Nakason C. Influence type of natural rubber on properties of green biodegradable thermoplastic natural rubber based on poly(butylene succinate). *Polym Adv Technol*. 2019;30:1010–1026. https://doi.org/10.1002/pat.4534